 

# A Structural Phase Transition and Molecular Motions in $(C_2H_5NH_3)_2[ZnBr_4]$ Studied by $^1H$ NMR and X-ray Diffraction

**Keizo Horiuchi,* Chieko Iijima,[1] Shinji Miyagi, Hayato Yogi, Takanori Fukami, and Ryuichi Ikeda[1]**

Faculty of Science, University of the Ryukyus, Nishihara-cho, Okinawa 903-0213

[1]Department of Chemistry, University of Tsukuba, Tsukuba 305-8571

Received May 31, 2004; E-mail: horiuchi@sci.u-ryukyu.ac.jp

The $^1H$ NMR spin–lattice relaxation times and the second moments of the resonance linewidth were measured as a function of temperature in $(C_2H_5NH_3)_2[ZnBr_4]$. The crystal structure at 295 K was determined to be orthorhombic with space group of $P2_12_12_1$ by the single-crystal X-ray diffraction method. The crystal undergoes a 1st order structural phase transition at $T_c = 300$ K, which is driven by the disordering of cationic orientations. The crystal structure above $T_c$ is inferred to be orthorhombic with space group of $Pmnb(D_{2h}^{16})$.

Bis-*n*-alkylammonium tetrahalogenozincates ($n$-$C_nH_{2n+1}NH_3)_2[ZnX_4]$ belong to the $A_2[MX_4]$ family with the $\beta$-$K_2SO_4$ structure (space group: $Pnma(D_{2h}^{16})$), where $MX_4^{2-}$ anion has a isolated tetrahedral structure. Many compouds in this family have already been extensively investigated; they show successive phase transitions and have incommensurate and/or ferroelectric phases.[1] We have already examined a temperature dependence of $^{81}Br$ nuclear quadrupole resonance (NQR) frequencies in $(C_2H_5NH_3)_2[ZnBr_4]$ above 77 K and have detected a first-order structural phase transition at $299.5 \pm 0.5$ K.[2] Furthermore, we have carried out calorimetric measurements between about 130 K and the melting point of 477 K and have detected a heat anomaly at $302 \pm 1$ K.[3,4] The observed transition entropy of $23 \pm 1.5$ J K$^{-1}$ mol$^{-1}$ suggests that this transition is of the order–disorder type. In the present invetigation, we have determined the crystal structure and the temperature dependences of the $^1H$ NMR spin–lattice relaxation time $T_1$ and the second moment $M_2$ of the resonance linewidth to study in detail the phase transition observed at 300 K in $(C_2H_5NH_3)_2[ZnBr_4]$.

## Experimental

The title compound was prepared by dissolving ethylamine and $ZnBr_2$ in hydrobromic acid with the stoichiometric ratio, and then by slowly evaporating water from the solution in a desiccator over $P_2O_5$. The crystal obtained was recrystallized from absolute ethanol by a slow-evaporation method. The sample was identified by elemental analysis. Anal. Calcd: C, 10.06; H, 3.35; N, 5.87%. Found: C, 10.02; H, 3.26; N, 6.00%.

A single-crystal X-ray diffraction was measured on a Nonius CAD-4 diffractometer with the graphite-monochromated Mo K$\alpha$ radiation ($\lambda = 0.71073$ Å) at 295 K. The intensity data were corrected for both Lorentz-polarization and absorption effects. The structure was solved by direct methods and refined by full-matrix least-squares methods. All of the calculations were performed on a VAX station 4000 with the MolEN program package.[5] The absolute structure was not determined. Hydrogen atoms were not located. Zn and Br atoms were refined with anisotropic thermal parameters and C and N atoms were refined with isotropic thermal parameters. Crystal data and experimental conditions are listed in Table 1. Crystallographic data have been deposited at the CCDC, 12 Union Road, Cambridge CB2 1EZ, UK and copies can be obtained on request, free of charge, by quoting the publication citation and the deposition number CCDC 252252. An X-ray powder diffraction was measured using Cu K$\alpha$ radiation ($\lambda = 1.542$ Å) with a Philips X'Pert-MPD and a Rigaku RINT-1500 diffractometer at 323 K.

The $^1H$ NMR spin–lattice relaxation time $T_1$ was measured by a Brucker SXP-100 spectrometer at a Larmor frequency of 40.0 MHz (89–395 K) and by a home-made pulsed spectrometer[6] at a frequency of 12.7 MHz (102–421 K). $T_1$ was determined by a $180^\circ$–$\tau$–$90^\circ$ pulse sequence. The second moment $M_2$ of the resonance linewidth was measured with a Brucker SXP-100 spectrometer at a Larmor frequency of 40.0 MHz using the solid-echo method[7] with a $90^\circ_x$–$\tau$–$90^\circ_y$ pulse sequence.

## Results and Discussion

**Crystal Structures.** Results of the crystal structure analysis are given in Tables 2 and 3 and in Fig. 1. Phases above and below the phase transition temperature are named high-temperature phase (HTP) and room-temperature phase (RTP), respectively. The results that a Laue group of *mmm* was accepted and that the systematic absences $h = 2n + 1$ for ($h$00), $k = 2n + 1$ for (0$k$0), and $l = 2n + 1$ for (00$l$) were recognized indicate that a possible space group is $P2_12_12_1$ in RTP. This space group is seldom observed in $A_2MX_4$ family with the $\beta$-$K_2SO_4$ structure (A = K, Rb, Cs, $NH_4$, and $(CH_3)_4N$, M = Mn, Fe, Co, Ni, Cu, Zn, Cd, and Hg); for a rare example, $P2_12_12_1$ was observed in $[(CH_3)_4N]_2[CoCl_4]$[8] and $[(CH_3)_4N]_2[ZnCl_4]$[9] as a commensurate phase at low temperature. This structure contains four crystallographically nonequivalent Br atoms in a unit cell: i.e., all of $ZnBr_4^{2-}$ in a unit cell are equivalent and four bromine atoms in a $ZnBr_4^{2-}$ are inequivalent, which is consistent with the fact that four resonance lines have been observed in $^{81}Br$ NQR.[2] The anions and cations make up repeated layers which are stacked alternately along the *c*-axis, as seen from Fig. 1. These two kinds of layers are connected by N–H···Br hydrogen bonds with lengths listed in Table 3. An X-ray powder diffraction

Published on the web December 10, 2004; DOI 10.1246/bcsj.77.2199

Table 1. Crystal Data, Data Collection, and Structure Refinement

| | | |
|---|---|---|
| Temperature/K | 295 | 323 |
| Crystal system | Orthorhombic | Orthorhombic |
| Space group | $P2_12_12_1$ | |
| $a$/Å | 7.696(1) | 7.72 |
| $b$/Å | 10.426(3) | 10.48 |
| $c$/Å | 17.757(9) | 17.84 |
| Volume of unit cell/Å | 1424.7(8) | 1443 |
| Formula unit per cell | 4 | |
| Density $D_x$/g cm$^{-3}$ | 2.225 | |
| $D_m$/g cm$^{-3}$ | 2.25(3) | |
| Linear absorption coefficient/mm$^{-1}$ | 25.721 | |
| Crystal size/mm$^3$ | $0.50 \times 0.47 \times 0.44$ | |
| Absorption correction type | Empirical via $\psi$ scans | |
| Transmission factor | 0.4608–0.9973 | |
| Number of reflections measured | 919 | |
| Number of independent reflections | 904 | |
| Number of reflectins used in refinement ($I \geq 3\sigma(I)$) | 352 | |
| Maximum value of $\theta$/deg | 20.97 | |
| $R$[a)] | 0.094 | |
| $wR$[a)] | 0.101 | |
| $S$ | 3.763 | |
| Number of parameters | 71 | |

a) Refinement on $F$.

Table 2. Fractional Atomic Coordinates and Equivalent Isotropic Displacement Parameters ($10^{-2}$ Å$^2$) in RTP, $U_{eq}$ is Defined as One Third of the Trace of the Orthogonalized $U_{ij}$ Tensor; $U_{eq} = \frac{1}{3}\sum_i \sum_j U_{ij} a_i^* a_j^* \mathbf{a}_i \cdot \mathbf{a}_j$

| Atom | $x$ | $y$ | $z$ | $U_{eq}$, $U_{iso}$ |
|---|---|---|---|---|
| Zn | 0.496(4) | 0.021(1) | 1.0437(5) | 6(1) |
| Br1 | 0.744(2) | −0.084(2) | 1.095(1) | 15(1) |
| Br2 | 0.510(3) | 0.243(1) | 1.0719(5) | 9(2) |
| Br3 | 0.491(7) | −0.013(1) | 0.9106(5) | 13(1) |
| Br4 | 0.244(1) | −0.0835(9) | 1.0937(7) | 6(3) |
| N1 | 0.54(1) | 0.317(6) | 0.883(3) | 5(9) |
| N2 | 0.03(1) | 0.869(8) | 0.932(4) | 9(9) |
| C11 | 0.56(1) | 0.32(1) | 0.802(6) | 10(10) |
| C12 | 0.43(1) | 0.25(1) | 0.763(5) | 7(3) |
| C21 | −0.04(2) | 0.88(1) | 0.862(7) | 17(2) |
| C22 | 0.03(1) | 0.925(9) | 0.796(5) | 9(2) |

Table 3. Bond Distances (Å), Angles (°), and N···Br Distances (Å) in RTP

| Bond distance | | Bond angle | | N···Br distance | |
|---|---|---|---|---|---|
| Zn–Br1 | 2.38(3) | Br1–Zn–Br2 | 109(1) | N1···Br1[a)] | 3.61(7) |
| Zn–Br2 | 2.37(1) | Br1–Zn–Br3 | 109(1) | N1···Br2[b)] | 3.78(8) |
| Zn–Br3 | 2.39(1) | Br1–Zn–Br4 | 107.4(6) | N1···Br2 | 3.45(6) |
| Zn–Br4 | 2.39(3) | Br2–Zn–Br3 | 110.7(5) | N1···Br3 | 3.50(7) |
| | | Br2–Zn–Br4 | 114(1) | N1···Br4[b)] | 3.22(7) |
| | | Br3–Zn–Br4 | 107(1) | N2···Br1 | 3.66(9) |
| N1–C11 | 1.4(1) | N1–C11–C12 | 114(8) | N2···Br1[a)] | 3.44(9) |
| C11–C12 | 1.4(1) | N2–C21–C22 | 119(13) | N2···Br3 | 3.8(1) |
| N2–C21 | 1.4(2) | | | N2···Br4 | 3.36(9) |
| C11–C12 | 1.5(1) | | | N2···Br4[a)] | 3.73(9) |

a) $x - 1/2, \bar{y} + 1/2, \bar{z} + 2$. b) $x + 1/2, \bar{y} + 1/2, \bar{z} + 2$.

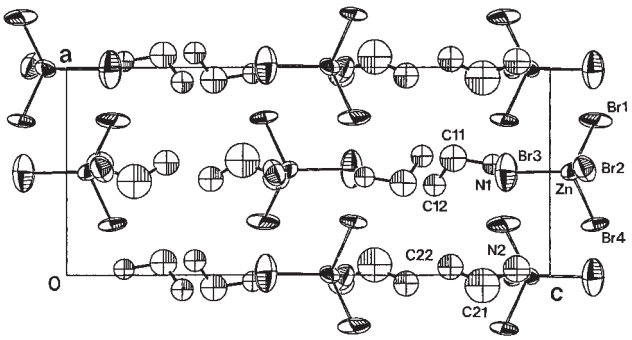


Fig. 1. A projection of the unit cell (RTP) onto the *ac* plane drawing by ORTEP with 50%-probability-displacement ellipsoids.

pattern taken at 323 K in HTP was well explained by an orthorhombic crystal system with $a = 7.72$, $b = 10.48$, and $c = 17.84$ Å. The systematic absences were not determined.

**Molecular Motions.** Temperature dependences of $^1$H NMR $T_1$ measured at 40.0 and 12.7 MHz are shown in Fig. 2. A cusp in the $T_1$ curve, i.e., a discontinuity of the temperature gradient of the $T_1$ curve, was observed at the phase transition temperature $T_c$. A large discontinuity in $T_1$ was not observed in $T_c$, although this phase transition is of first order. The observed $T_1$ curve gave a minimum around 150 K and a Larmor-frequency dependence only on the low-temperature side of $T_1$ minimum. This temperature dependence is attributable to the magnetic dipolar relaxation caused by thermal molecular motions, and can be analyzed by the BPP equation[10] using the Arrhenius relationship between the motional correlation time $\tau_c$ and the motional activation energy $E_a$, as given by

$$\tau_c = \tau_{c0} \exp\left(\frac{E_a}{RT}\right). \quad (1)$$

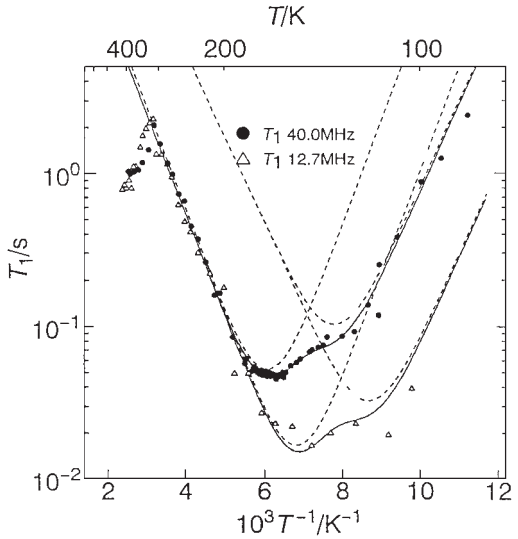


Fig. 2. Temperature dependences of $^1$H NMR $T_1$. Solid curves are the best-fitted calculated values. Broken curves are contributions from respective molecular motions (see text).

Table 4. Activation Energies $E_a$, Pre-Exponential Factors $\tau_{c0}$, and Motional Modes of Ethylammonium Cations Determined from $^1$H $T_1$ Data

| Phase | $E_a$ /kJ mol$^{-1}$ | $\tau_{c0}$ /$10^{-13}$ s | Motional mode |
|---|---|---|---|
| RTP | 10.8 | 1.0 | $CH_3$ rotation |
| | 12.9 | 2.0 | $NH_3^+$ rotation |
| HTP | | | Axial rotation |

The obtained best fit $T_1$ curves are displayed in Fig. 2 and the determined values of motional parameters are listed in Table 4. The assignment of motional modes was carried out by calculating $M_2$ values.[11] Since proton positions could not be located by the crystal structure analysis, the calculation was performed by assuming proton positions using standard values for an alkyammonium ion.[12]

The decrease in $T_1$ with increasing temperature observed in HTP suggests that a new motion other than the $CH_3$ and $NH_3^+$ rotations is excited above the transition temperature. We assigned it to the hindered axial rotation of the whole cations about the molecular long axes because, in $(n\text{-}C_5H_{11}NH_3)_2[ZnCl_4]$ and $(n\text{-}C_{12}H_{25}NH_3)_2[ZnCl_4]$, the axial rotation of the whole alkyl chain was found,[13] and the observed transition entropy $\Delta S$ of 23 J K$^{-1}$ mol$^{-1}$ is well explained by this motion. If an order–disorder type of transition occurs in connection with the orientation of $C_2H_5NH_3^+$ ions, the $\Delta S$ experimentally observed can be interpreted in terms of the Boltzmann principle

$$\Delta S = 2R \ln(N_H/N_R), \quad (2)$$

where, $N_H$ and $N_R$ are the number of distinguishable orientations allowed in HTP and RTP, respectively. Since the present crystal-structure analysis shows that $C_2H_5NH_3^+$ cations are ordered in RTP, $N_R = 1$. Hence, the observed $\Delta S$ value of 23 J K$^{-1}$ mol$^{-1}$ leads to $N_H = 4$. This value is well explained by the hindered axial rotation of the cations.

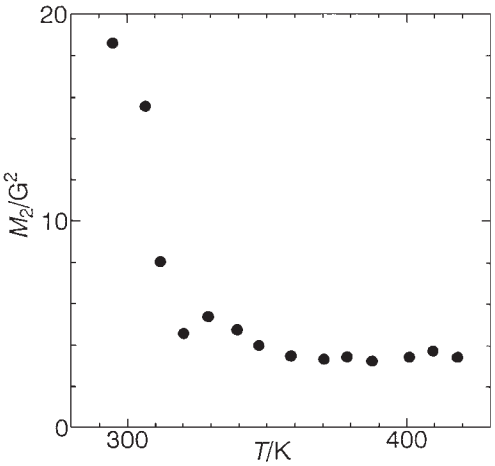


Fig. 3. A temperature dependence of the second moment $M_2$ of $^1$H NMR absorptions.

The temperature dependence of $M_2$ in the range 294–418 K is represented in Fig. 3. $M_2$ values in HTP were abruptly reduced to ca. 6 G$^2$ from ca. 18 G$^2$ just below the transition temperature in RTP and finally reduced to a constant value of ca. 3.6 G$^2$, implying the onset of a new motion in HTP that averages most of the protonic dipolar interactions. It is the axial rotation of rigid cations about their molecular axes that is responsible for the large $M_2$ reduction observed. However, the axial rotation leads to the calculated $M_2$ value of ca. 7 G$^2$, which is much larger than the observed value. The new motion in HTP is expected to be dynamically more disordered than the uniaxial rotation, and this disorder can be attributed to the orientational distribution (i.e., the random tumbling or the precessional motion) of the cationic axis about the crystallographic $c$-axis.

**Phase Transition.** From the DSC and NMR results, we can conclude that the phase transition at 300 K in $(C_2H_5NH_3)_2[ZnBr_4]$ is driven by the disordering of ethylammonium orientations. The dynamic disordering of cations about the molecular long axes means that the cations can obtain a higher molecular symmetry. For example, the disorder can produce mirror planes at cation sites. $Pmnb(D_{2h}^{16})$ requies mirror planes at (100) and (200) on the $P2_12_12_1$ lattice. If ethylammonium cations are dynamically disordered, they can be located on the mirror planes in the $Pmnb$ lattice, as can be seen from Fig. 1. The anions can also be located on the mirror planes with a small displacement. Hence, the space group of HTP is expected to be $Pmnb(D_{2h}^{16})$. In fact, the crystal structure at room temperature in $(C_2H_5NH_3)_2[ZnCl_4]$ is reported to be $Pnma(D_{2h}^{16})$,[14] although the detailed crystal structure data and/or figures are unavailable. Although a $Pmcn(D_{2h}^{16})$–$P2_1/c(C_{2h}^5)$ transition is frequently observed in $A_2[MX_4]$ family with the $\beta$-$K_2SO_4$ structure (A = K, Rb, Cs, $NH_4$, and $(CH_3)_4N$, M = Mn, Fe, Co, Ni, Cu, Zn, Cd, and Hg), a $Pmnb$–$P2_12_12_1$ transition is not observed in this system, as far as we know. On the other hand, a $Pnma(D_{2h}^{16})$–$P2_12_12_1(D_2^4)$ transition is observed in $(C_2H_5NH_3)_2[ZnCl_4]$[14] and $(n\text{-}C_5H_{11}NH_3)_2[ZnCl_4]$.[15] This phase sequence is considered to be characteristic of bis-$n$-alkyammonium tetrahalogenozincates $(n\text{-}C_nH_{2n+1}NH_3)_2ZnX_4$.

## Conclusion

$(C_2H_5NH_3)_2[ZnBr_4]$ was shown to form an orthorhombic structure with space group of $P2_12_12_1$ at 295 K. It undergoes a 1st order structural phase transition at 300 K, which is driven by the dynamical disordering of ethylammonium orientations along their long axes. This may be a $Pmnb(D_{2h}^{16})$–$P2_12_12_1(D_2^4)$ transition. $C_2H_5NH_3^+$ cations perform the hindered axial rotation about the molecular long axes that randomly distribute or perform a precessional motion about the crystallographic *c*-axis above 300 K.

This work was partly supported by Grant-in-Aid for Scientific Research No. 06640450 from the Ministry of Education, Culture, Sports, Science and Technology.

## References

1 "Incommensurate Phases and Dielectrics," ed by R. Blinc and A. P. Levanyuk, Amsterdam, North-Holland (1986).

2 K. Horiuchi and A. Weiss, *J. Mol. Struct.*, **345**, 97 (1995).

3 K. Horiuchi, *J. Phys. Soc. Jpn.*, **63**, 363 (1994).

4 Y. Sakiyama, K. Horiuchi, and R. Ikeda, *J. Phys.: Condens. Matter*, **8**, 5345 (1996).

5 C. K. Fair, "MolEN, An Interactive Intelligent System for Cryatal Structure Analysis," Delft, Enraf-Nonius (1990).

6 T. Kobayashi, H. Ohki, and R. Ikeda, *Mol. Cryst. Liq. Cryst. Sci. Technol.*, **257**, 279 (1994).

7 J. G. Powles and J. H. Strange, *Proc. Phys. Soc., London*, **82**, 6 (1963).

8 S. Sawada, T. Yamaguchi, H. Suzuki, and F. Shimizu, *J. Phys. Soc. Jpn.*, **54**, 3136 (1985).

9 S. Sawada, T. Yamaguchi, H. Suzuki, and F. Shimizu, *J. Phys. Soc. Jpn.*, **54**, 3129 (1985).

10 N. Blomembergen, E. M. Purcell, and R. V. Pound, *Phys. Rev.*, **73**, 679 (1948).

11 J. H. Van Vleck, *Phys. Rev.*, **74**, 1168 (1948).

12 "Kagakubinran," 4th ed, ed by Japan Chemical Society, Maruzen, Tokyo (1993).

13 K. Horiuchi, H. Takayama, S. Ishimaru, and R. Ikeda, *Bull. Chem. Soc. Jpn.*, **73**, 307 (2000).

14 A. G. Cuevas, J. M. P. Mato, M. J. Tello, G. Madariaga, J. Fernandez, L. Echarri, F. J. Zuniga, and G. Chapuis, *Phys. Rev.*, **B29**, 2655 (1984).

15 M. J. Tello, A. Lopez-Echarri, J. Zubillaga, I. Ruiz-Larrea, F. J. Zuniga, G. Madariaga, and A. Gomez-Cuevas, *J. Phys.: Condens. Matter*, **6**, 6751 (1994).